SAND-79-0126C
CONF-791016--35

MASTER

MEDIUM-SCALE MELT-SODIUM FRAGMENTATION UNDER INERTIA

T. Y. Chu, A. C. Bentley,
W. D. Krotning and L. A. Powers

Sandia Laboratories
Albuquerque, New Mexico 87185

NOTICE

ABSTRACT

The results of a series of fragmentation experiments involving up to 20 Kg of thermitically produced high temperature melts and 23 Kg of sodium are presented. Except for one experiment where some centimeter size particles are observed, the fragment distributions seem to be in the range of previous data. Spatial distribution of the fragments in the debris bed appears to be stratified. Scanning electron micrographs of fragments indicate fragmentation to be occurring in the molten state for the more intense interactions observed. Interaction data obtained show quiescent periods of 0.5 - 1.5 second between pressure pulses. The force impulse values per unit mass of melt seems to be in the same range as previous experiments.

INTRODUCTION

Several accident sequences involve the contact between molten reactor material and coolant. The nature of the fuel fragment debris resulting from this contact strongly influences the coolability of the debris and the subsequent probability of remelting as a threat to the containment system. The current experimental program is designed to try to determine the mode of fuel fragmentation and the characteristics of the resulting debris, and to provide the initial condition for debris bed dryout studies [1]. Related measurements may also provide information on possible interactions that convert portions of the thermal energy to mechanical energy.

The experiments executed to date and currently underway typically utilize ~20 Kg each of sodium and high-temperature melt produced by metallothermic reactions. Experimental fragmentation results involving such large quantities of material are currently limited and scaling effects are not well understood [2].

DISTRIBUTION OF THIS DOCUMENT IS UNLIMITED

The program consists of three general classes of experiments: melt streaming into sodium (forward), sodium into melt (reverse), and combined interaction experiments. Experiments in the last class utilize a concrete vessel to determine the effect of sodium-concrete interaction on fragmentation as a result of gas generation, creation of entrapment sites, and possible triggering of FCI due to pressure pulses produced by sodium-concrete interactions.

The present paper summarizes the currently available results of the melt into sodium (forward) experiments.

DESCRIPTION OF TESTS

A schematic of the apparatus for the forward (melt into sodium) experiment is shown in Figure 1. The top section houses the metallothermic mixture in a sillimanite crucible inside a steel vessel. The melt is released by a melt-out channel plug; the melting time of the plug provides a time delay allowing the venting of gaseous reaction products. The melt is monitored by a γ ray densitometry device, by a pyrometer and by photography. The sodium-crucible assembly consists of an inner magnesium oxide vessel 34 cm I.D. and 46 cm deep with an outer thick bottom stainless steel vessel. Tubular heaters surrounding the vessel are used to heat the sodium. There are thermocouples in the sodium pool and embedded in the bottom of the crucible. Pressure measurement is made through a side port on the sodium vessel. Three force transducers on the vessel bottom provide force measurements. An acoustic transducer at the end of a steel bar immersed in the sodium pool is used to monitor the acoustic emission of the interaction. Motion picture and television recording with audio coverage from a microphone next to the apparatus are made of each test.

Post-test examination of the fragments includes: bulk fragment size analysis, core sample study of debris bed structure, scanning electron micrograph study of the size, shape and compositions of fragments and fragment density measurements.

RESULTS

The test conditions for the experiments to be discussed are summarized in Table 1. Two of the tests utilized a thermically produced iron/Al_2O_3 (44 W/O) melt and the other three used a stainless steel/UO_2, ZrO_2 (70 W/O) corium like melt. Other variables were stream size (13 mm - 51 mm) and sodium temperature (250 C - 690 C).

Interaction Results

In none of the tests was a single coherent energetic event observed; rather, the interactions were all characterized by a series of pressure events occurring throughout the time period corresponding to the draining

of the melt crucible. In the FRAG 2 test the interaction was of sufficient intensity to cause some mechanical damage to the test apparatus.

Visual observation during FRAG 2 showed that the thermal events lasted approximately 5 seconds and five loud acoustic signals were recorded by the microphone next to the apparatus. Coincident with the next to the last signal the entire assembly weighing 1000 Kg was observed to jump 1.7 cm and the vessel head plate (Figure 1), 1.3 cm thick and 65 cm in diameter, was bowed 0.5 cm. Peak interaction pressure exceeded the transducer range of 20 bar. Typical width of the pressure pulses and force pulses were, respectively, 300 μsec and 8 msec. From the pulse width and rise rate, the peak pressure in FRAG 2 was estimated to be 50-100 bar. The interaction data from pressure, force and acoustic measurements are displayed and compared in Figure 2. Since the limits of transducer response and the playback device were exceeded, the pressure and force peaks displayed do not accurately reflect the maximum pressures experienced. The entry of the melt, zero time, is marked by a sharp rise of the acoustic emission. Temperature data indicated that the melt reached the pool bottom (20 cm deep) without being totally dispersed. There were no appreciable pressure pulses until 1.1 sec after the initial entry of the melt. All the data traces showed exact correspondence in time as well as a resemblance in shape. There appeared to be periods (.5 - 1.5 sec) of quiescence between pulses. This seems to be typical of all the test data available to date. The γ ray densitometry data showed an apparent increase in density corresponding to each pressure peak indicating that sodium gases were injecting the vessel head with each pressure event. This was apparently the cause of the head deformation and the jump of the vessel. The minimum ideal impulses for the head deformation was calculated [3] to be 214 N-sec (48 lb_f-sec).

Some estimates of the impulses from the force traces of the transducer located on the bottom of the sodium vessel were made for FRAG 6. A total of nine separate force pulses were observed. The values of each individual impulse ranges from approximately 45 N-sec to 530 N-sec. M3 experiment from Argonne National Laboratory [4] used a 1.4 Kg of melt and 3.0 Kg of sodium at 900 K (627 C), reported five pulse ranging from 0.45 N-sec (0.1 lb_f-sec) to 19.6 N-sec (4.4 lb_f-sec). On a per unit mass of melt basis the biggest impulses are within approximately a factor of two (present experiment being higher). The total sums of the impulses per unit mass of melt are also within approximately a factor of two.

Fragment Analysis

The fragments from each experiment are classified by size. Scanning electron micrographs and chemical analyses are made to determine the structure and chemical composition of the fragments. Density measurements are also made of the fragments using both helium pycnometry and water pycnometry; these measurements together with fragment weight fraction in the bed give the void fraction of the debris bed.

Thus far the debris of FRAG 2 and FRAG 4 has been analyzed by sieving

for particle sizes larger than 45 μm. The distribution of finer fragments were obtained by sedimentation (Micrometrics Sedigraph 5 %) down to 0.2 μm; a sonic sifter is also used to classify fragments down to 5 μm. As shown in Figure 3, both size distributions are approximately log-normal. Significant deviation to the log-normal distribution starts to occur for sizes below the 50-100 μm range. This trend seems to be typical of a number of previous experiments. Since the melts for the two tests are different, no direct comparison can be made. However, FRAG 4 distribution does show good agreement with the data of M series tests [3] of ANL. The median size particle is 320 μm. The distributions of finer fragments obtained by sedimentation are shown in Figure 4. Since the mass fraction of particles less than 45 μm is 1.0% for FRAG 2 and 0.4% for FRAG 4, 100% on the plot corresponds to 1% and 0.4% of the total fragment mass for each experiment respectively. Calculated from the results in Figure 4, approximately 0.6% of the particles are less than 10 μm and 2.0% are less than 1 μm for FRAG 2 and approximately 7.2% of the fragments are less than 10 μm and 2.1% are less than 1 μm for FRAG 4. Density measurements were made of the sieved particles from FRAG 2 (Al_2O_3 and iron melt). Except for the largest particles, there is a general trend of decreasing density with particle size. A plausible explanation is that Al_2O_3 is more easily fragmented; therefore, there is a larger ratio of Al_2O_3 in fine fragments. The measurements are being repeated and the fragments are being chemically analyzed for composition.

Scanning electron micrographs (S.E.M.) of FRAG 1 and FRAG 2 tests are displayed in Figure 5 to show the relation between the fragment structure and the intensity of interaction. Both tests utilize an iron/alumnia melt. The iron appears to be white in the photograph and alumnia appears to be gray. FRAG 1 was relatively mild and the fragments are all single phase. A great number of alumina fragments have a jagged outline indicating fragmentation due to stress. FRAG 2 fragments are more smooth in appearance. They are mostly two phase with spheriodal or nearly speriodal inclusions of the other phase. These fragments give a vivid picture of molten materials being fragmented and intermixed. Since fragmentation occurred in the molten state, post-test examination of the particle size may not be indicative of the size responsible for the interaction. Coalescence as well as further fragmentation obviously occurred as a result of interactions. S.E.M. photographs of fragments from FRAG 4 are shown in Figure 6; there are both single and multi-phase particles and there are large number of fragments with internal voids. The bulk density of the fragments was measured to be 4.9 g/cm^3. This value is less than the density of stainless steel as well as the oxides further confirming the existance of the internal voids.

In the first four experiments (FRAG 1 - FRAG 5) the MgO reaction vessel was always cracked but there was never any indication of damage due to melt attack. However, in FRAG 6, the crucible bottom showed evidence of melt attack. In a region of approximately 16 cm in diameter (crucible diameter is 34 cm the melt stream diameter is 5.1 cm) the crucible bottom showed depth of attack of up to 0.6 cm. Since the surface of the melt

attacked region appears to be pitted rather than smooth, the attack is at least partly due to thermal stress. However, further analysis of the fragments is required to provide more information concerning the nature of the melt attack. Apparently the high sodium temperature (696 C) resulted in a more stable boiling around the melt mass, thus allowing the melt to remain to be a more coherent mass in going through the 28 cm depth of sodium and reaching the bottom of the reaction vessel. This is also consistent with the fact that FRAG 6 was the only experiment in the present series where fragments of several centimeters in size were observed, Figure 7.

Debris Bed Structure

Core samples were made of the debris bed from each test and the spatial distribution of the fragments were examined. Data available to date shows that the spatial particle size distribution is stratified; i.e., the large particles are more likely to be found near the bottom. Such a configuration should produce a more coolable bed than one with uniform particle distribution. The degree of stratification appeared to be greatest for the test in which the intensity of the pressure events was greatest. Particle size classification is yet to be made of core samples as a function of position to further quantify these observations.

Core samples were sectioned into 13 mm to 19 mm intervals and the weight of each section is measured before and after the removal of sodium to obtain the fragment weight fraction as a function of height. The results from FRAG 4 and FRAG 5 are shown in Figure 8. The lower part of the bed has essentially constant weight fraction. The top portion of the beds show a gradual and smooth transition from this constant value to essentially zero weight fraction within a distance of about 50 mm. The size stratification is most pronounced within the transition region. The upper portion of the transition zone cannot really be considered to be part of the "debris bed", since the particle concentration is in no way enough to form a self supporting porous structure. The finer particles were probably in suspension due to the convective motion. Using the measured fragment bulk density of 4.9 g/cm^3 for FRAG 4, the void fraction of the lower part of the bed is calculated to be 50%.

SUMMARY

Results of fragmentation experiments involving up to 20 Kg of thermitically produced high temperature melts and 23 Kg of sodium are presented. Except for one experiment where some centimeter size particles are observed, the fragment distributions seem to be in the range of previous data. Spatial distribution of the fragments in the debris bed appears to be stratified. Scanning electron micrographs of fragments indicate fragmentation to be occurring in the molten state for the more intense interactions observed. Interaction data obtained show quiescent periods of 0.5 - 1.5 second between pressure pulses. The force impulse values per unit mass of melt seems to be in the same range as previous experiments.

REFERENCES

1. Rivard, J.B., Debris Bed Studies and Experiments at Sandia Laboratories SAND78-0299, Sandia Laboratories, 1978.

2. Board, C.J. and L. Caldarola, Fuel-Coolant Interaction in Fast Reactors Annual ASME Winter Meeting: Nuclear Reactor Safety Heat Transfer Section, Atlanta, Georgia, November 27-December 2, 1977, pp.195-223.

3. Longcope D.B., Sandia Laboratories, Private Communication

4. Johnson, T.R., L. Baker, Jr., and J.F. Pavlik, "Large-Scale Molten Fuel-Sodium Interaction Experiments," Proc. Fast Reactor Safety Meeting April 2-4, 1974, Beverly Hills, California, CONF-74-401-p2, p.683.

5. Gluekler, E.L. and L. Baker, Jr., Post-Accident Heat Removal in LMFBR's ASME Winter Meeting: Nuclear Reactor Safety Heat Transfer Section, Atlanta, Georgia, November 27-December 2, 1977, pp. 265-324.

ACKNOWLEDGMENTS

This work was performed under the auspices of the United States Nuclear Regulatory Commission.

The authors acknowledge the help of Alfred Angel of Sandia Laboratories in carrying out the experiments.

	FRAG 1	FRAG 2	FRAG 4	FRAG 5	FRAG 6
STREAM SIZE MM	13	51	51	51	51
MELT	FE AL_2O_3 (44%)	FE AL_2O_3 (44%)	UO_2-ZRO_2 (70%) STAINLESS STEEL	UO_2-ZRO_2 (70%) STAINLESS STEEL	UO_2-ZRO_2 (70%) STAINLESS STEEL
MELT MASS KG	12	13	20	20	20
SODIUM KG	23	23	23	23	23
SODIUM TEMPERATURE °C	520	480	420	250	690
MAX. OBSERVED PRESSURE BAR	2	> 20	- - -	2	7
MECHANICAL DAMAGE	NO	YES	NO	NO	NO

TABLE I - SUMMARY OF EXPERIMENTS PERFORMED

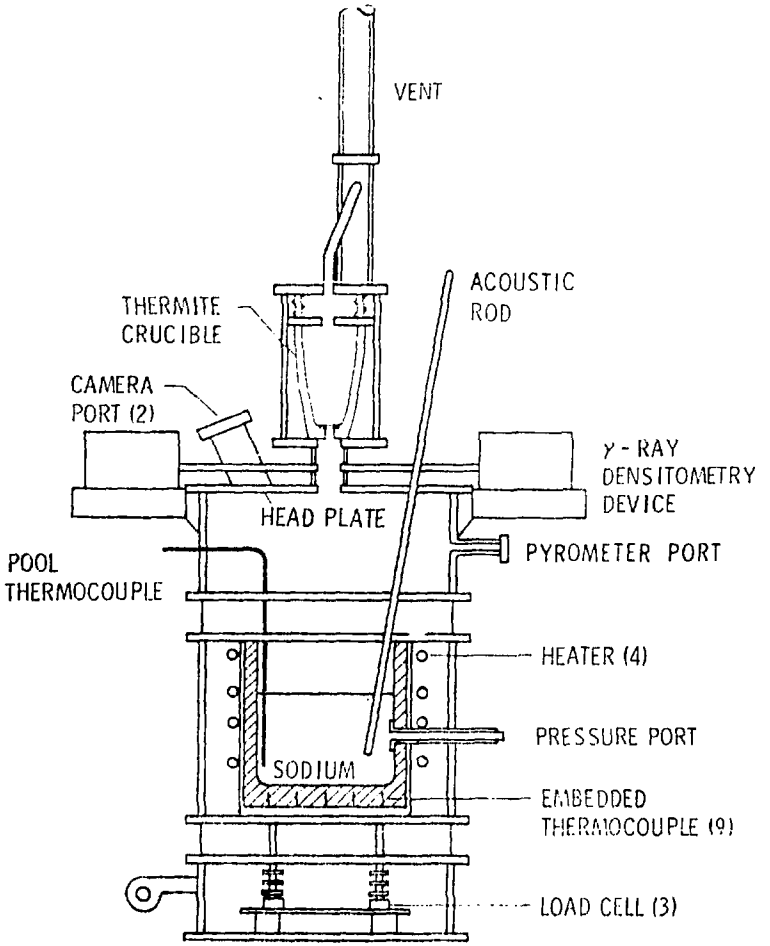
VENT
ACOUSTIC ROD
THERMITE CRUCIBLE
CAMERA PORT (2)
γ - RAY DENSITOMETRY DEVICE
HEAD PLATE
POOL THERMOCOUPLE
PYROMETER PORT
HEATER (4)
PRESSURE PORT
SODIUM
EMBEDDED THERMOCOUPLE (9)
LOAD CELL (3)

Fig. 1

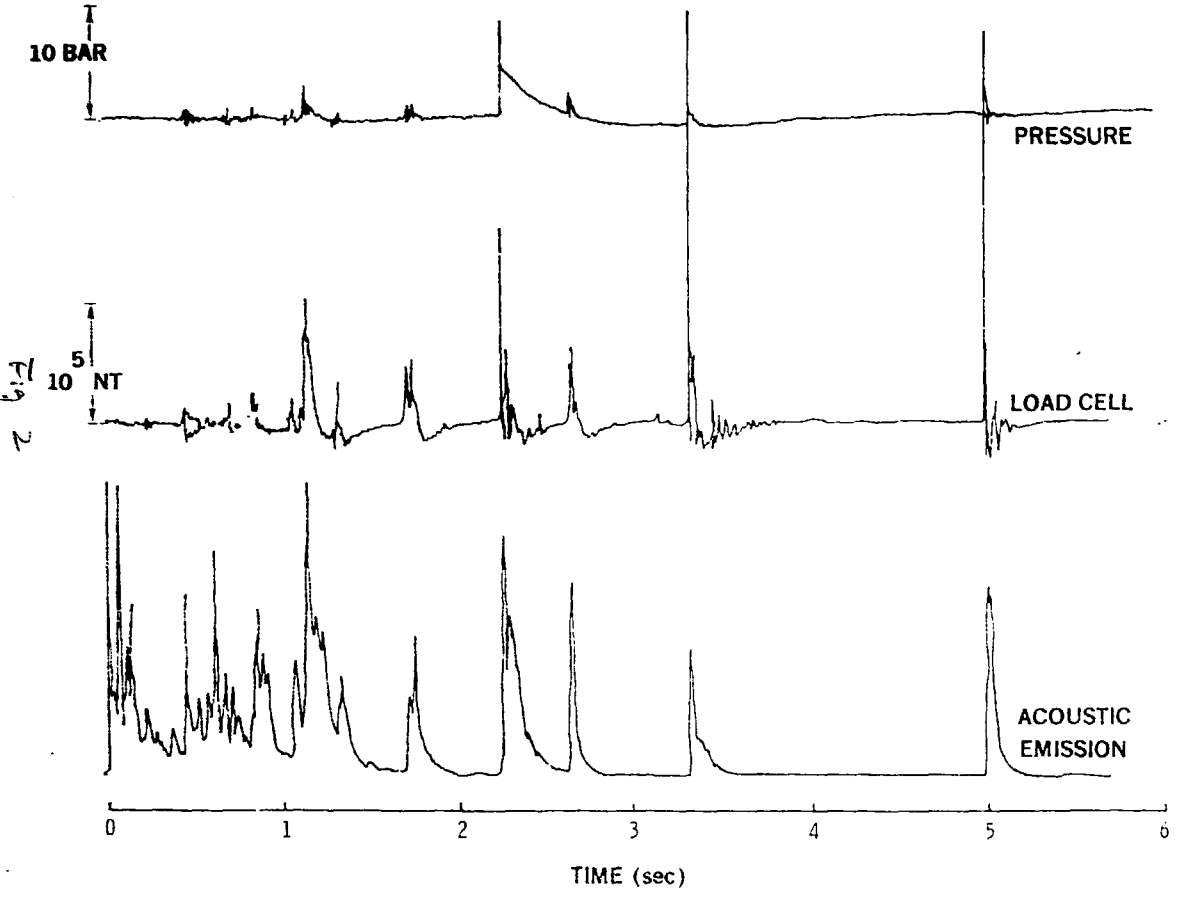
10 BAR
PRESSURE
10^5 NT
LOAD CELL
ACOUSTIC
EMISSION
0
1
2
3
4
5
6
TIME (sec)

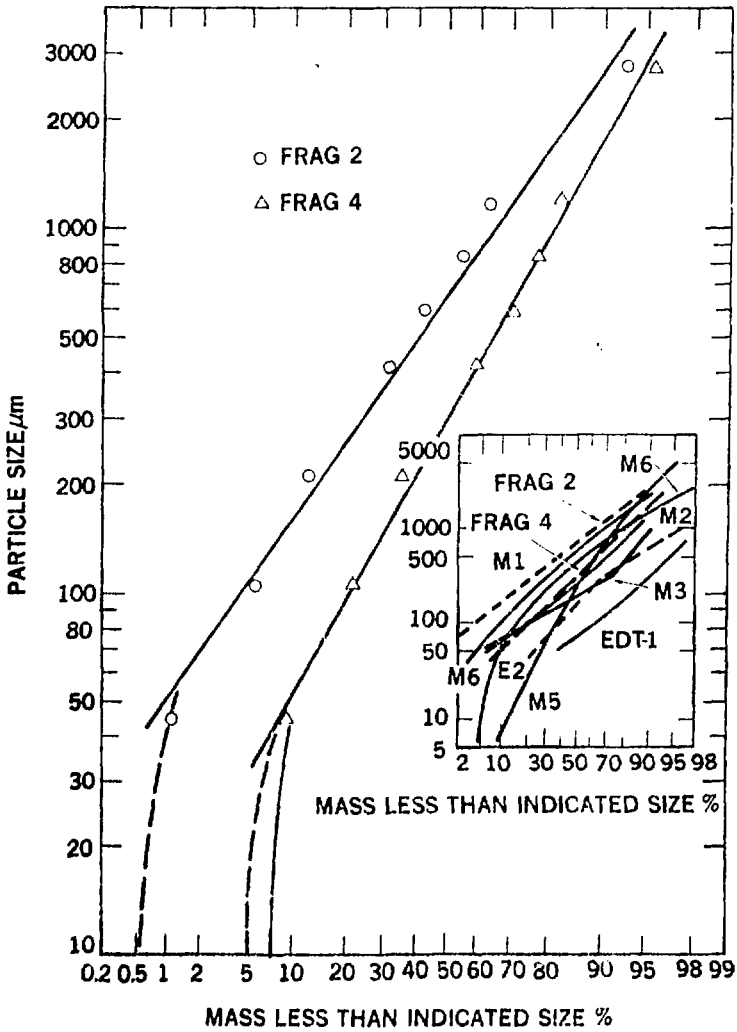
PARTICLE SIZE μm
3000
2000
1000
800
500
300
200
100
80
50
30
20
10
FRAG 2
FRAG 4
0.2 0.5 1 2 5 10 20 30 40 50 60 70 80 90 95 98 99
MASS LESS THAN INDICATED SIZE %
5000
1000
500
100
50
10
5
FRAG 2
FRAG 4
M1
M2
M3
M5
M6
E2
EDT-1
2 10 30 50 70 90 95 98
MASS LESS THAN INDICATED SIZE %

Fig 3

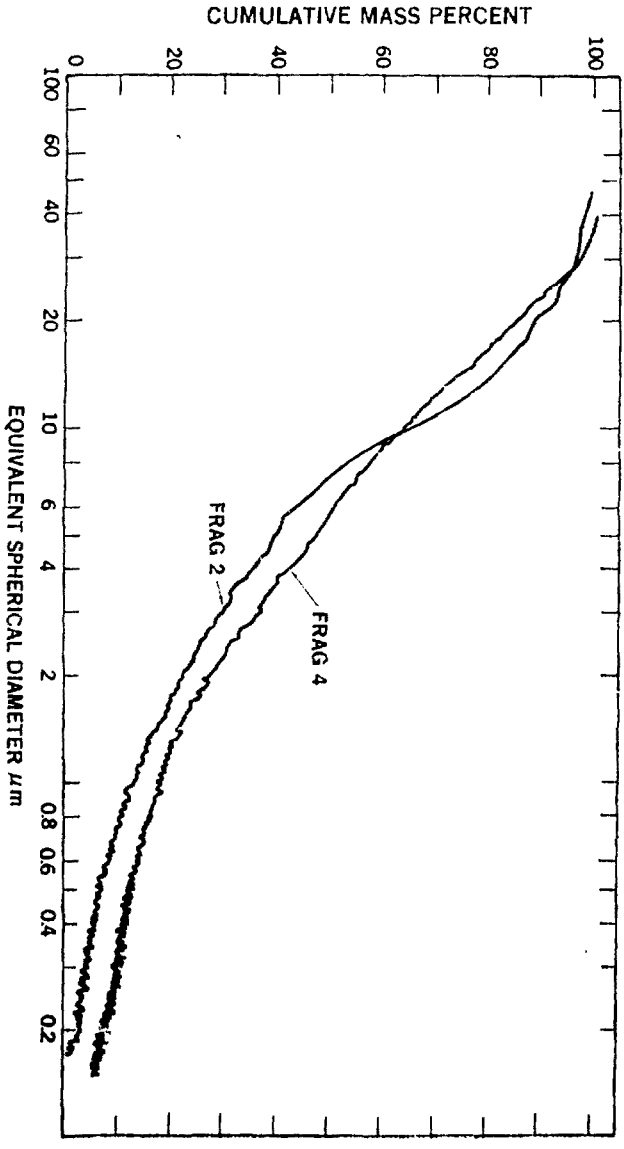
CUMULATIVE MASS PERCENT
0
20
40
60
80
100
100
60
40
20
10
6
4
2
0.8
0.6
0.4
0.2
EQUIVALENT SPHERICAL DIAMETER μm
FRAG 2
FRAG 4

Fig 4

FRAG 1

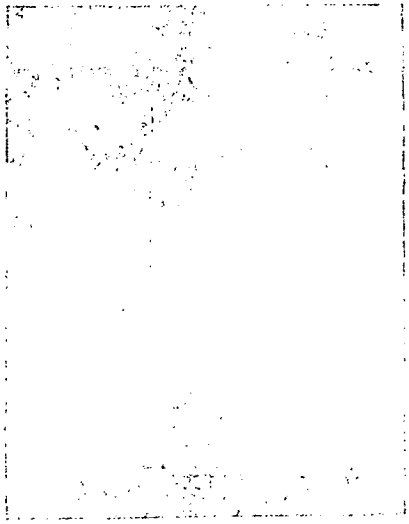

FRAG 2

FRAG 2

Fig 5

FRAG 4

FRAG 4

Fig 6

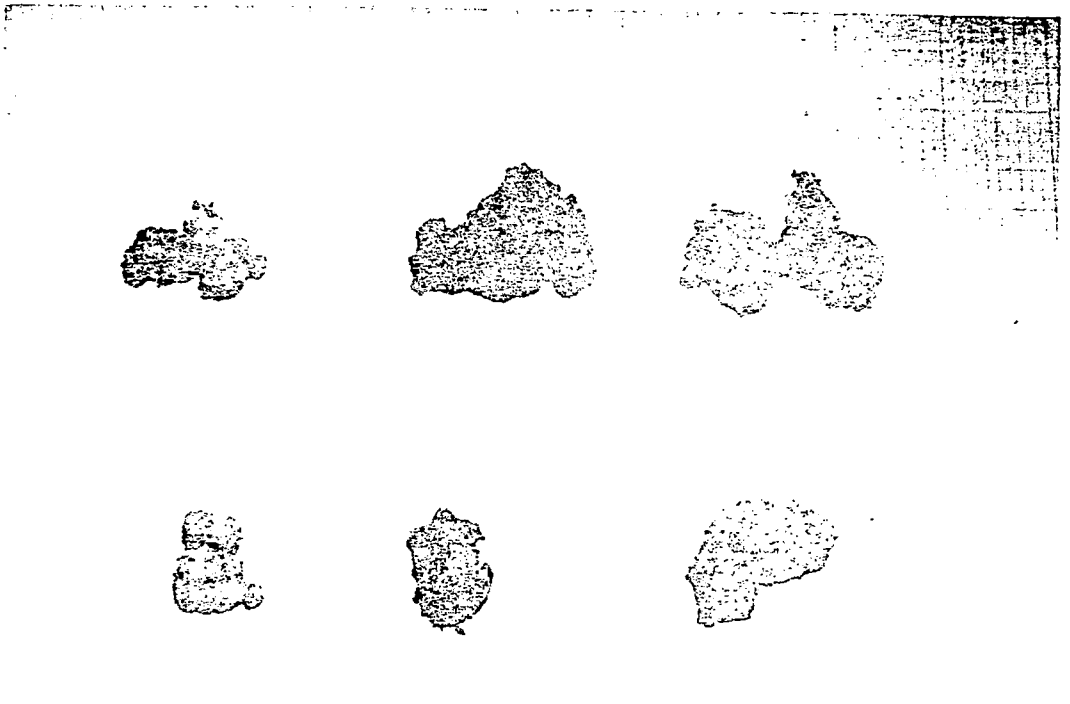

F87

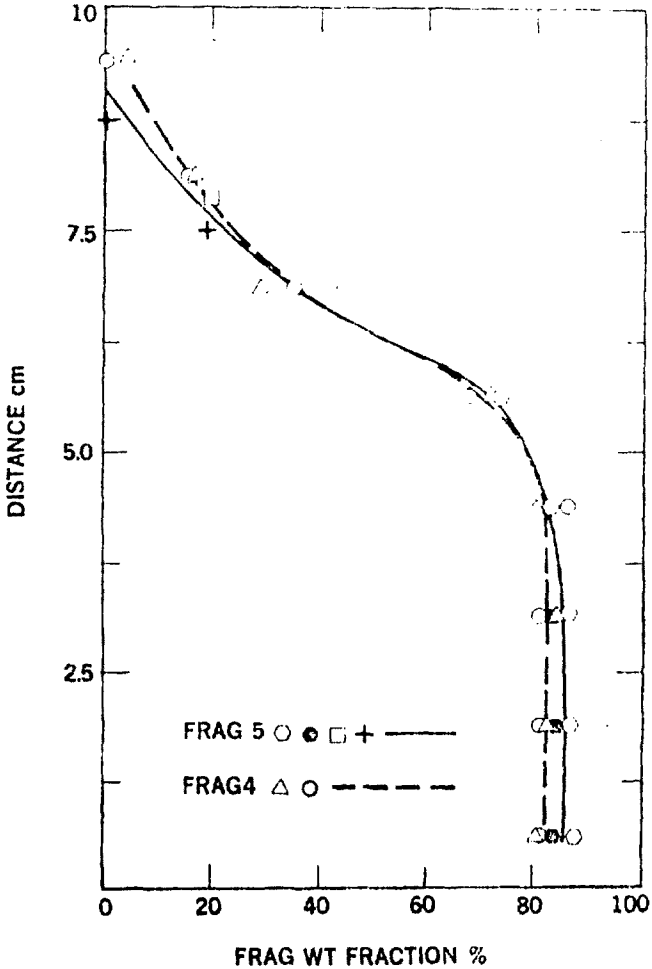
10
7.5
5.0
2.5
DISTANCE cm
0
20
40
60
80
100
FRAG WT FRACTION %
FRAG 5 ○ ● □ + ——
FRAG4 △ ○ — — —

Fig 8